

Heavy fermion fluid in high magnetic fields: an infrared study of $\text{CeRu}_4\text{Sb}_{12}$

S. V. Dordević^{1,2}, K. S. D. Beach², N. Takeda³, Y. J. Wang⁴, M. B. Maple¹, and D. N. Basov¹

¹ Department of Physics, University of California, San Diego, La Jolla, CA 92093

² Department of Physics, Boston University, Boston, MA 02215

³ Institute for Solid State Physics, University of Tokyo, 5-1-5 Kashiwa, Chiba 277-8581, Japan and

⁴ National High Magnetic Field Laboratory, Tallahassee, FL 32310

(dated: December 29, 2021)

We report a comprehensive infrared magneto-spectroscopy study of $\text{CeRu}_4\text{Sb}_{12}$ compound revealing quasiparticles with heavy effective mass, with a detailed analysis of optical constants in fields up to 17 T. We find that the applied magnetic field strongly affects the low energy excitations in the system. In particular, the magnitude of m^* (m_b is the quasiparticle band mass) at 10 K is suppressed by as much as 25% at 17 T. This effect is in quantitative agreement with the mean-field solution of the periodic Anderson model augmented with a Zeeman term.

PACS numbers: 72.15.Jf, 75.20.Hr, 78.30.Hr

Systematic investigations of physical properties of Heavy Fermion (HF) materials have provided valuable insights into the role played by many-body effects in transport and magnetic phenomena [1]. The HF ground state is believed to be a manifestation of a delicate balance between competing interactions [2]. External stimuli can readily tip the balance yielding a variety of novel forms of matter. Motivated by the exceptional richness and complexity of effects occurring in the HF systems under applied external stimuli, many research teams have undertaken the methodical investigation of properties under the variation of relevant control parameters, such as pressure (P) or magnetic field (H) [3, 4, 5]. In this work we focused on the analysis of the low energy excitations of the HF system $\text{CeRu}_4\text{Sb}_{12}$ in high magnetic field using infrared (IR) spectroscopy. This technique has emerged as a very powerful experimental probe of the HF ground state [6, 7]. Essentially all hallmark features of the HF state, such as the quasiparticle effective mass, the optical gap, and a narrow Drude-like peak (with the width $1/\tau$) can be simultaneously studied based on the analysis of the optical constants.

Our IR magneto-optics results uncover robustness of the HF fluid in $\text{CeRu}_4\text{Sb}_{12}$ against magnetic field: a field of 17 T suppresses the quasiparticle effective mass by about 25%. The reason we selected $\text{CeRu}_4\text{Sb}_{12}$ for high-field investigations reported here is two-fold. First, the family of skutterudite compounds to which $\text{CeRu}_4\text{Sb}_{12}$ belongs reveals a broad spectrum of behavior, including non-Fermi liquid power laws, superconductivity with unconventional order parameter and antiferromagnetism [8, 9, 10, 11]. This catalogue of enigmatic properties supports the notion of the competing ground states: a regime where even modest external stimuli are likely to have a major impact on the response of a system. Second, our earlier zero-field experiments have uncovered remarkably large changes of reflectance $R(\omega)$ of $\text{CeRu}_4\text{Sb}_{12}$ at low temperatures: the reflectance drops by more than 20% in the far-IR [7]. With such a strong feature, unprecedented

among HF compounds, a task of monitoring subtle field-induced modifications of electrodynamics is becoming a viable endeavor.

Samples of $\text{CeRu}_4\text{Sb}_{12}$ were synthesized using Sb flux method with an excess of Sb (for more details on sample growth see Ref. 8). Large polycrystalline specimens with a typical surface area of 4 cm^2 were essential for magneto-optical experiments. The samples have been characterized by resistivity and magnetization measurements and found to be of similar quality as previously reported [8].

The electrodynamic response of $\text{CeRu}_4\text{Sb}_{12}$ was studied using infrared and optical reflectance spectroscopy. Zero-field near-normal incidence reflectance $R(\omega)$ was measured in the frequency range $30\text{--}30,000\text{ cm}^{-1}$ (approximately $4\text{ meV--}4\text{ eV}$) from $T=10\text{ K}$ to room temperature. These measurements were supplemented with magneto-optic reflectance ratios $R(\omega, H)/R(\omega, H=0\text{ T})$ obtained in zero-field cooling conditions at 10 K [12]. The absolute value of reflectance in magnetic field $R(\omega, H)$ was obtained by multiplying these ratios with the $H=0$ data $R(\omega, H) = [R(\omega, H)/R(\omega, H=0\text{ T})] R(\omega)$. The complex optical conductivity $\sigma(\omega) = \sigma_1(\omega) + i\sigma_2(\omega)$ and dielectric function $\epsilon(\omega) = \epsilon_1(\omega) + i\epsilon_2(\omega)$ were obtained from reflectance using Kramers-Kronig analysis. For low-frequency extrapolations, we used the Hagen-Rubens formula (thin line in Fig. 1). The overall uncertainty in $\sigma_1(\omega)$ and $\sigma_2(\omega)$ due to low- and high-frequency extrapolations required for Kramers-Kronig analysis is about 8–10%. This uncertainty does not affect any conclusions of the paper in any significant way.

Plotted in the top panel of Fig. 1 is the temperature dependence of reflectance $R(\omega)$ over an extended frequency interval. The gross features of $R(\omega)$ are in good agreement with the spectra obtained previously on single crystals [7]. The general shape of the reflectance spectrum at 300 K is metallic, with high absolute values at low frequencies, and a well defined edge around $4,000\text{ cm}^{-1}$ (not shown). Below a coherence temperature T^* which

is about 50 K for $\text{CeRu}_4\text{Sb}_{12}$ [7] there is a strong suppression of reflectance in the range between 50 and 1,000 cm^{-1} . This result is indicative of the development of a gap in the density of states commonly observed in HF systems. Simultaneously a new feature develops in the far-IR. This structure bears similarities with the conventional "plasma edge" in metals and is established as a spectroscopic signature of heavy quasiparticles [6]. The reflectance edge softens with decrease of T down to 60 cm^{-1} in the 10 K spectra. Several narrow peaks in the far-IR region are due to optically active phonons and will be discussed below.

The bottom panel of Fig. 1 displays the reflectance data in magnetic field, plotted on a linear scale over a narrower frequency interval in order to emphasize field-induced changes. Only a few in-field curves are shown for clarity. For comparison, the plot also includes several zero-field spectra at higher temperatures. The thin line is a Hagen-Rubens extrapolation used for the 300 K spectrum. For fields below 5 T no significant change in reflectance can be detected, within the error bars of the experiment. At higher fields, the frequency position of the low-lying "plasma edge" hardens, a behavior which is paralleled by zero-field spectra taken at higher T . Comparing temperature- and field-induced modification of $R(\omega)$, we notice that the net effect of applying a 17 T field is functionally equivalent to a temperature increase of 20 K. At higher frequencies ($\omega > 110 \text{ cm}^{-1}$) the reflectance is field independent for $H < 17 \text{ T}$, within the error bars of the present experiment.

The top panel of Fig. 2 displays the temperature dependence of the dissipative part of the optical conductivity $\sigma_1(\omega)$. The dominant feature in the low- T data is a sharp increase in the conductivity above 80 cm^{-1} with an overshoot of the 300 K spectrum at 550 cm^{-1} . This behavior is usually assigned to the formation of the (hybridization) gap in the excitation spectrum of a HF system [6]. Because of the improved signal-to-noise ratio, it became possible to extend earlier zero-field measurements [7] to lower frequencies. These new results allow us to resolve the onset of a narrow Drude-like feature, usually associated with the response of heavy quasiparticles at low T [6]. The gradual suppression of the conductivity at $\omega < 60 \text{ cm}^{-1}$ at low T is consistent with the decrease of the quasiparticle scattering rate $1/\tau(\omega)$ below the low- ω cut-off of our data (30 cm^{-1}). The latter effect will lead to an increase of the conductivity in the $\omega \rightarrow 0$ limit, in accord with the DC resistivity measurements [9, 10, 13] displayed with full symbols. The narrow resonances at 88, 116, 131, 205, 221 and 248 cm^{-1} are phonon modes. Some of these modes, including the peaks at 88, 131 and 205 cm^{-1} , have not been observed before in measurements on smaller single crystals [7]. We also observe an additional mode at 40 cm^{-1} which can be identified only in the low- T spectra once the electronic background in the conductivity is diminished.

The bottom panel of Fig. 2 displays the optical conductivity $\sigma_1(\omega)$ at 10 K in a magnetic field, along with 30 K data (in zero field). Only a limited frequency region is shown to emphasize the effects due to applied fields. We find that the onset of the gap structure in $\sigma_1(\omega)$ is virtually unaffected even by the 17 T field. On the other hand, the coherent mode due to heavy quasiparticles broadens as the field increases. This is consistent with positive magneto-resistance in the DC data [9, 10, 13].

Field induced effects in the optical constants can be quantified using several complementary methods. The extended Drude model (EDM) offers an instructive analysis protocol and is routinely used to quantify correlation effects in HF systems [6]. Within the EDM the optical constants are expressed in terms of the quasiparticle scattering rate $1/\tau(\omega)$ and the effective mass spectrum $m(\omega)$ [6]. Specifically, $m(\omega)$ can be obtained from the following equation:

$$\frac{m(\omega)}{m_b} = \frac{\omega_p^2}{4\omega} \text{Im} \frac{1}{\epsilon(\omega)}; \quad (1)$$

where $\omega_p = \frac{1}{4\pi\epsilon_0 n} = 10,744 \text{ cm}^{-1}$ is the plasma frequency estimated from the integration of $\sigma_1(\omega)$ up to the frequency of the onset of interband absorption. The spectra of $m(\omega)$ in HF compounds usually reveal a complicated frequency dependence which is particularly true in the vicinity of the energy gap [6]. However, an extrapolation of $m(\omega)$ spectra towards zero frequency yields a reliable estimate of the quasiparticle effective mass m^* that has been shown to agree with the thermodynamic mass for a variety of HF compounds [6, 7]. The estimated value of $0.70 m_b$ (at 10 K) $\text{CeRu}_4\text{Sb}_{12}$ is somewhat smaller than previously reported $80 m_b$ for single crystals [7]. This effect can be assigned to increased disorder and/or variations of the Kondo temperature in polycrystalline specimens compared with previously studied single crystals. In the middle panel of Fig. 3 we plot the extracted values of the mass in zero frequency limit as a function of magnetic field. A 17 T field is capable of suppressing the mass by about 25% from its zero-field value.

Alternatively, mass renormalization can be inferred from the analysis of the loss function spectra $\text{Im}[1/\epsilon(\omega)]$ (top panel of Fig. 3). The loss function offers a convenient way to explore longitudinal modes in the optical spectra, including heavy electron plasmons in HF compounds [6]. These longitudinal modes produce Lorentzian-like peaks in $\text{Im}[1/\epsilon(\omega)]$ spectra centered at $\omega_p = \frac{1}{4\pi\epsilon_0 n} m^*$, where ϵ_1 is the high-frequency contribution to the dielectric function. In Fig. 3 the plasmon due to heavy quasiparticles is clearly observed at 0.74 cm^{-1} at 10 K. As temperature increases the plasmon shifts to higher energies, implying a decrease of the quasiparticle effective mass ($m^* \propto 1/\tau(\omega)$). Similarly, as the magnetic field

increases, the mode hardens to 90 cm^{-1} , which again indicates that the heavy quasiparticles reduce their effective mass. In the top panel of Fig. 3, we plot the field dependence of the mass determined from the frequency of the peak in the loss function spectra. In full agreement with the values obtained by extrapolating $m^*(\omega)$ spectra to zero frequency, we observe a marked depression of the effective mass by nearly 25% at 17 T, with the characteristic downward curvature.

We have also employed two additional methods of quantifying the field-induced changes of m^* . The simplest estimate of renormalization is the (inverse of the) position of the minimum in reflectance. The minimum in reflectance, the so-called plasma minimum, is determined by the screen plasma frequency, which on the other hand is proportional to the ratio n/m^* , where n is the carrier density and m^* their effective mass. The plasma minimum points (from Fig. 1) are also plotted in the middle panel of Fig. 3 and they agree well with previous two data sets. Finally the partial sum rule:

$$\int_0^{\omega_c} \omega^2 \epsilon''(\omega) d\omega = \frac{(\epsilon_p^0)^2}{8} = \frac{ne^2}{2m^*}; \quad (2)$$

can also give an estimate of the effective mass [6]. The upper integration limit ω_c was set just below the onset of hybridization gap. The values of the effective mass extracted this way are also in good agreement with the other three methods (Fig. 3, middle panel). The scatter of data points in Fig. 3 serves as an estimate of the error bars.

The Periodic Anderson Model (PAM) is believed to capture the essence of the physics in HF metals [1]. We will show below that this model when augmented with the Zeeman term elucidates the behavior of the effective mass in a magnetic field. At the mean-field level, the heavy fermion state is characterized by hybridization of the free (c) and localized (f) electrons [14, 15]. Hybridization breaks the conduction band into disjoint upper and lower branches with very shallow dispersion near the gap edge (Fig. 3 bottom panel); this accounts for the very large effective mass of the quasiparticles. The state is metallic and possesses a well-defined Fermi surface that incorporates both the c and f electrons. In the presence of a Zeeman term (which consists of a magnetic field H coupled to the total magnetic moment at each site) the mass enhancement factor behaves as [16]:

$$\frac{m^*}{m_e} = \frac{m}{m_e} \left(1 + 2s \frac{H}{H_0} + \frac{3}{2} \frac{H^2}{H_0^2} \right); \quad (3)$$

where m_e is the free electron mass, $s = \langle \sigma^2 \rangle / \langle \sigma \rangle$ and H_0 is on the order of the Kondo energy in magnetic units. The linear term in Eq. 3 results from the splitting of the Fermi surface into separate spin-up and spin-down surfaces, each with a different band curvature. The

quadratic term is due to higher-order changes in the hybridization energy.

The quasiparticle contribution to the optical conductivity $\sigma_1(\omega)$ of the Zeeman-split heavy electron metal is:

$$\sigma_1(\omega) = \frac{e^2}{m_e} \frac{X}{s} \frac{n_s}{1 - i\Gamma(\omega = m_e)s}; \quad (4)$$

where Γ is the quasiparticle scattering rate. The quasiparticles have a total density $n = n^* + n_{\#} = n_c + n_f$; in a Zeeman field, they are spin-polarized according to $n^* - n_{\#} = H/H_0$. In the limit $H \rightarrow 0$, Eqs. 3 and 4 can be combined to give:

$$\frac{\epsilon_p^2}{4} \text{Im} \frac{1}{\sigma_1(\omega)} = \frac{m}{m_e} \left(1 + \frac{5}{2} \frac{2n_f}{n} \frac{H}{H_0} \right)^2; \quad (5)$$

which for $H = 0$ T reduces to Eq. 1. According to Eq. 5, the effective mass probed in an IR experiment is averaged between the two spin channels and its magnitude is reduced as $(H/H_0)^2$, in full agreement with the experimental observation (top panel of Fig. 3). The ϵ_p (gray line) corresponds to $H_0 = 35$ T. This estimate of H_0 is lower than the Kondo temperature $T_K \approx 100$ K [10] for $\text{CeRu}_4\text{Sb}_{12}$ but is close to the coherence temperature $T^* \approx 50$ K. The Zeeman splitting also implies an overall reduction of the energy gap between the spin-down sub-band at $E > E_F$ and the spin-up sub-band at $E < E_F$ [16]. As pointed out above, appreciable reduction of the gap is not observed in our data. This is consistent with the notion that in an optical experiment one probes separately gaps in the spin-up and spin-down channels, provided that spin- $\uparrow\downarrow$ scattering does not significantly alter the selection rules. Neither of the two transitions is expected to significantly change in fields smaller than the hybridization gap. Further theoretical studies are needed to address the issue of spin- $\uparrow\downarrow$ scattering, as well as the problem of the field dependence of the hybridization energy.

In conclusion, we have presented a comprehensive set of infrared data obtained on $\text{CeRu}_4\text{Sb}_{12}$ in high magnetic field. The external field is found to affect the low-energy excitations of the system, which leads to the renormalization of the quasiparticle effective mass. Indeed, a 17 T field was found to diminish m^* by about 25%. Mean-field solution of the PAM with a Zeeman term offers a quantitative account for the field dependence of the effective mass.

The research supported by NSF.

^YPresent Address: Department of Physics, The University of Akron, Akron, OH 44325

FIG. 1: Temperature and field dependence of the resistance of $\text{CeRu}_4\text{Sb}_{12}$. Top panel: temperature dependence with $H = 0$. Bottom panel: high field resistance at $T = 10\text{ K}$, along with several zero field curves at higher temperatures.

FIG. 2: Temperature and field dependence of the real part of the optical conductivity $\sigma_1(\omega)$. Top panel: temperature dependence in zero field. Bottom panel: optical conductivity in high magnetic field at $T = 10\text{ K}$, along with several zero field curves at higher temperatures.

- [1] A.C. Hewson, *The Kondo Problem to Heavy Fermions*, (Cambridge University Press, 1997).
- [2] S.Doniach, *Physica B* 91, 231 (1977).
- [3] P.Gegenwart et al., *J. Low Temp. Phys.* 133, 3 (2003).
- [4] K.H.Kim et al. *PhysRevLett.* 91, 256401 (2003).
- [5] N.Harrison, M.Jaime and J.A.Miyoshi, *PhysRevLett.* 90, 096402 (2003).
- [6] L.Degorgi, *RevModPhys.* 71, 687 (1999).
- [7] S.V.Dordevic, D.N.Basov, N.R.Dilley, E.D.Bauer and M.B.Mapple, *PhysRevLett.* 86, 684 (2001).
- [8] N.Takeda and M.Ishikawa, *Physica B*, 259–261, 92, (1999).

- [9] N.Takeda and M.Ishikawa, *Physica B* 281{282, 388 (2000).
- [10] E.D.Bauer et al., *JPhys:CondensMatter* 13, 5183 (2001).
- [11] E.D.Bauer et al. *PhysRevB* 65, 100506 (2002).
- [12] W.J.Padilla, Z.Q.Li, K.S.Burch, Y.S.Lee, K.J.Mikolajitis and D.N.Basov, *Rev.Sci.Instrum.* 75, 4710 (2004).
- [13] K.Abe et al., *JPhys:CondensMatter* 14, 11757 (2002).
- [14] P.Coleman, *PhysRevB* 35, 5072 (1987).
- [15] A.J.Millis and P.A.Lee, *PhysRevB* 35, 3394 (1987).
- [16] K.S.D.Beach, cond-mat/0509778.

FIG. 3: The top panel presents the loss function $\text{Im}[1/\epsilon(\omega)]$, which has pronounced peaks at the frequencies of the longitudinal modes, such as the heavy plasmon ω_p . All field curves are at $T = 10\text{ K}$. The middle panel shows the field dependence of quasiparticle effective mass m^* extracted from: 1) the $m^*(\omega)$ spectra, 2) the maximum in the loss function $\text{Im}[1/\epsilon(\omega)]$, 3) minimum in resistance $R(\omega)$ and 4) the integral of the narrow Drude mode (Eq. 2). The bottom panel schematically displays the PAM band structure, both in zero and high magnetic field.

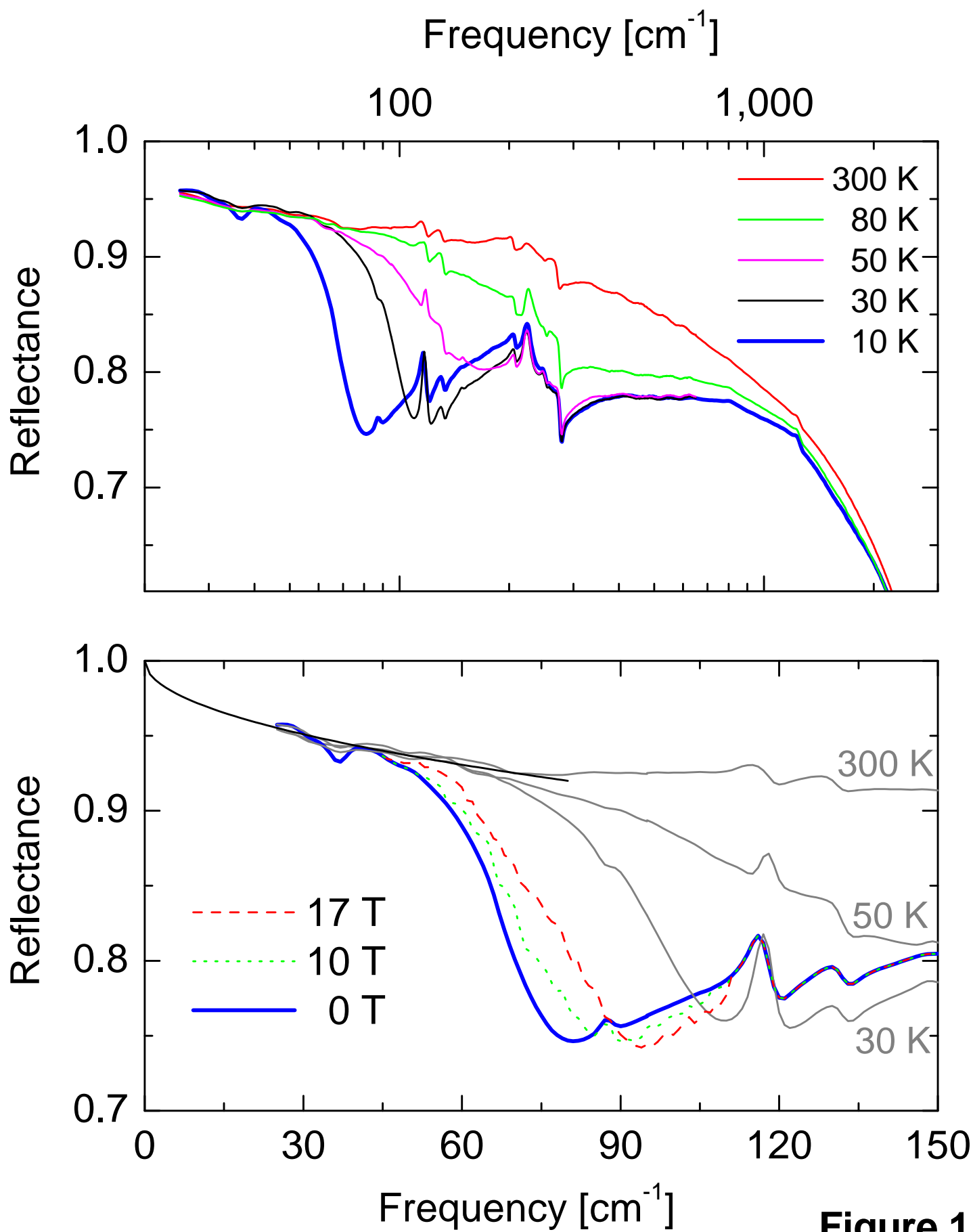
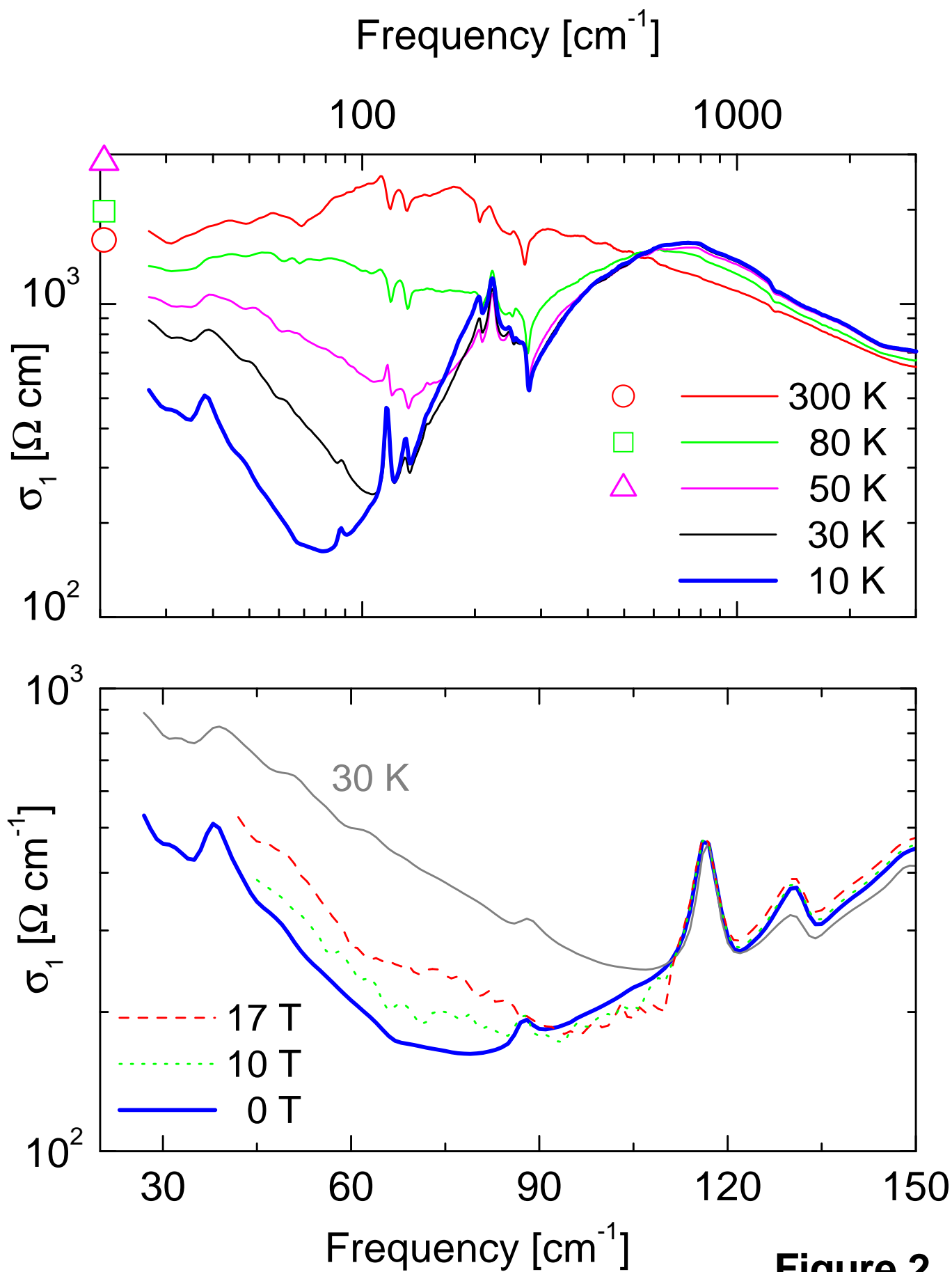


Figure 1



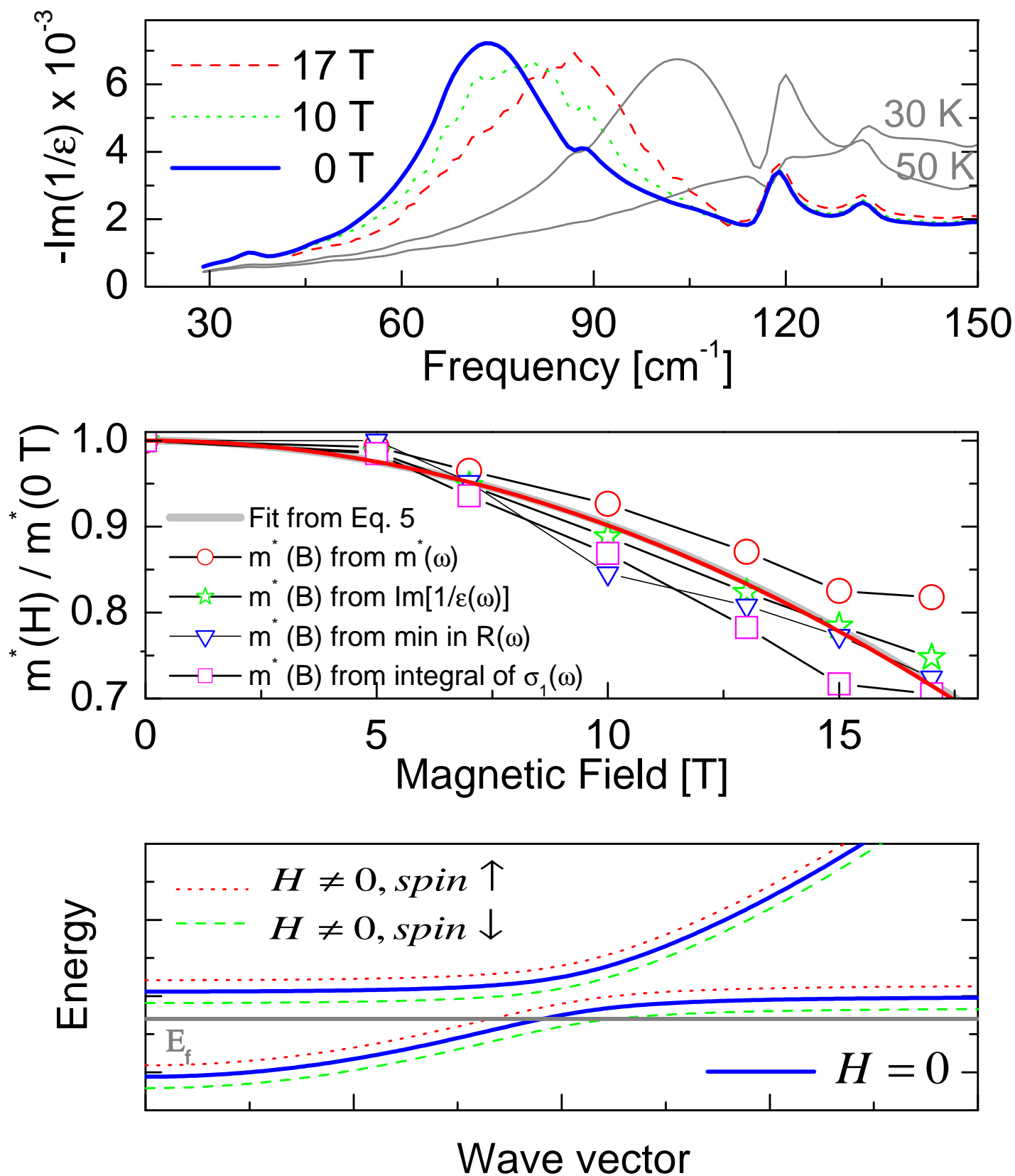


Figure 3